EDGEWOOD

CHEMICAL BIOLOGICAL CENTER

U.S. ARMY SOLDIER AND BIOLOGICAL CHEMICAL COMMAND

ECBC-TR-328

RELATIONSHIP OF AMBIENT ATMOSPHERE AND BIOLOGICAL AEROSOL RESPONSES FROM A FIELDED PYROLYSIS-GAS CHROMATOGRAPHY-ION MOBILITY SPECTROMETRY BIOANALYTICAL DETECTOR

A. Peter Snyder
Waleed M. Maswadeh

RESEARCH AND TECHNOLOGY DIRECTORATE

Ashish Tripathi

GEO-CENTERS

GEO-CENTERS, INC. - GUNPOWDER BRANCH

December 2003

Aberdeen Proving Ground, MD 21010-5424

DISCLAIMER

The findings in this report are not to be construed as an official Department of the Army position unless so designated by other authorizing documents.

REPORT DOCUMENTATION PAGE

Form Approved
OMB No. 0704-0188

1. AGENCY USE ONLY *(Leave Blank)*	2. REPORT DATE	3. REPORT TYPE AND DATES COVERED
	2003 December	Final; 01 Mar – 01 Oct

4. TITLE AND SUBTITLE
Relationship of Ambient Atmosphere and Biological Aerosol Responses from a Fielded Pyrolysis-Gas Chromatography-Ion Mobility Spectrometry Bioanalytical Detector

5. FUNDING NUMBERS
PR-

6. AUTHOR(S)
Synder, A., Peter; Maswadeh, Waleed M. (ECBC); and Tripathi, Ashish (GEO-CENTERS, INC.)

7. PERFORMING ORGANIZATION NAME(S) AND ADDRESS(ES)
DIR, ECBC, ATTN: AMSRD-ECB-RT-DD, MD 21010-5424
GEO-CENTERS, INC., P.O. Box 68, Gunpowder Branch, APG, MD 21010-0068

8. PERFORMING ORGANIZATION REPORT NUMBER
ECBC-TR-328

9. SPONSORING/MONITORING AGENCY NAME(S) AND ADDRESS(ES)

10. SPONSORING/MONITORING AGENCY REPORT NUMBER

11. SUPPLEMENTARY NOTES

12a. DISTRIBUTION/AVAILABILITY STATEMENT
Approved for public release; distribution is unlimited.

12b. DISTRIBUTION CODE

13. ABSTRACT *(Maximum 200 words)*
Interrogation of the ambient atmosphere for identification of bioaerosol material has predominately been accomplished by aerosol particulate collection, concentration, and growth on agar plates coupled with biochemical tests. A challenge facing the aerobiological community is characterizing the ambient atmospheric aerosol burden with respect to a relatively rapid monitoring for distinct biological species. A pyrolysis-gas chromatography-ion mobility spectrometry stand-alone bioaerosol system was interfaced to an aerosol concentrator to collect ambient background aerosols and produce bioanalytical baseline/background signal levels over 28-hr. Random, discrete, deliberate bursts of biological aerosol near the aerosol concentrator inlet were performed during the continuous bioanalytical interrogation of an outdoor urban atmospheric environment. In the presence of outdoor aerosol background, detection, classification, and characterization of the bioaerosol were accomplished from relatively low to high concentration aerosol bursts of Bacillus subtilis spores and ovalbumin protein. This work provides initial attempts to shepherd continuous bioanalytical instrumentation monitoring of the ambient atmospheric aerosol for detection and classification of specific bioaerosols.

14. SUBJECT TERMS
Ion Mobility Spectrometry
Bacillus subtilis spores
Gas chromatography
Bacteria aerosols
Outdoor aerosol collection
Field detection
Biodection
Pyrolysis

15. NUMBER OF PAGES
33

16. PRICE CODE

17. SECURITY CLASSIFICATION OF REPORT	18. SECURITY CLASSIFICATION OF THIS PAGE	19. SECURITY CLASSIFICATION OF ABSTRACT	20. LIMITATION OF ABSTRACT
UNCLASSIFIED	**UNCLASSIFIED**	**UNCLASSIFIED**	**UL**

Blank

PREFACE

The work described in this report was authorized under Project No._____. This work was started in March 2001 and completed in October 2001.

The use of either trade or manufacturers' names in this report does not constitute an official endorsement of any commercial products. This report may not be cited for purposes of advertisement.

This report has been approved for public release. Registered users should request additional copies from the Defense Technical Information Center; unregistered users should direct such requests to the National Technical Information Center.

Blank

CONTENTS

FIGURES

RELATIONSHIP OF AMBIENT ATMOSPHERE AND BIOLOGICAL AEROSOL RESPONSES FROM A FIELDED PYROLYSIS-GAS CHROMATOGRAPHY-ION MOBILITY SPECTROMETRY BIOANALYTICAL DETECTOR

1. INTRODUCTION

Interrogation of the ambient atmosphere for the presence of biological material has predominately been accomplished by aerosol particulate collection, concentration, and growth on agar plates. This system of bioaerosol analysis has been performed to investigate and delineate the atmospheric aerosol burden of biological entities such as fungal spores, bacteria, and viruses for purposes such as health of communities, containment, forecasting of disease in agriculture, aerobiological monitoring for compliance guidelines, exposure limits, and general atmospheric dispersion trends.[1-3] Visual analysis of the biological growth on selective media in agar plates is commonly used to characterize the content of a collected bioaerosol.[4-7] A taxonomic status of the concentrated bioaerosol can be obtained by using standard microbiological tests that include growth observation, morphology, staining, biochemical, and specific enzyme tests.[5, 7, 8] Classification and identities of biological species found in atmospheric bioaerosols can be obtained by these simple yet powerful methods of agar plate growth coupled with biochemical tests. The scientific community has performed these methods for over half a century, and the methods have been used for monitoring various outdoor environments during daily, weekly, monthly, and yearlong intervals.[4, 7, 8-14] Databases have been generated that provide historical records for correlation on what type of atmospheric biological burden may exist at a given locale for the time of day and season.[8, 15] It was a primary intention of these extensive studies and methods to provide for an off-line analysis for the general and more specific, taxonomic status of the sampled ambient background air. These methods are necessarily time and labor intensive.

During the past decade, a number of developments occurred on the continuous outdoor monitoring of the overall ambient biological burden with analytical and bioanalytical instrumentation. Noteworthy techniques can be found in the spectroscopy and spectrometry sciences. Laser excitation with UV-VIS fluorescence monitoring of bioaerosols provide biological event detection information,[16-20] and pyrolysis-gas chromatography-ion mobility spectrometry (Py-GC-IMS) provided biological event detection as well as some details on the type of biological species present in the aerosol.[21-23] Deliberately-released bioaerosols in an outdoor prairie environment were interrogated with Py-mass spectrometry (MS). Even though it is in its preliminary stages, Py-MS offers a promising bioanalytical dimension in that characterization of fatty acid mass signatures were evident for Gram positive spores and Gram negative bacterial aerosols.[24] These systems cannot yield the detailed taxonomic information that results from the agar plate and biochemical test approaches. Details about the identity or identities of a significant portion of the biological species in background ambient air appear to be beyond the scope of spectroscopy and spectrometry instrumentation without extensive and time-consuming microbiological separation and biochemical processing techniques. However, the spectroscopy and spectrometry systems can provide biological event detection and general

classification information and overall trends/changes in the ambient bioaerosol burden. This information may be accomplished in a continuous monitoring mode where either instrument or detection process is repetitively cycled.

It is well known that polymerase chain reaction (PCR)[3, 25-27] and immunochemical, antigen-antibody methods[3, 28] can be applied to studying the bioaerosol burden in ambient atmospheres; however, their application is used mainly for discrete, off-line samples as opposed to an on-line, continuous monitoring format. The spectroscopy and spectrometry techniques (*vide supra*) do not use biological molecule reagent expendables for detection and identification.

Lighthart[4] offers the aerobiological monitoring community eight major challenges that require further investigation. One of these challenges is the "evaluation of the interference of natural atmospheric bacterial phenomena with surveillance and detection of airborne bacterial agents." Lighthart[9] adds, "Today there are in addition other practical problems regarding ... evaluation of present day atmospheric microbial loads to determine the extent of microbial air pollution levels and to develop atmospheric microbial detection instrumentation in which natural background microorganisms might obscure specific anthropogenic agents, e.g., microbiological pest control agents and biological warfare agents." Additional literature in the field provides thought-provoking ideas that are similar in concept.[2, 3, 10]

The present study attempts to address these important concepts in aerobiological monitoring by building on the foundation of bioaerosol event detection with a Py-GC-IMS system. An aerosol concentrator was interfaced to the pyrolysis (rapid heating) sample introduction module of the briefcase-sized Py-GC-IMS system. The pyrolysis source consists of a Pyrex tube with a quartz frit to capture the aerosol particulates. The aerosol is drawn onto the frit by an internal pump. A wire coil on the outside of the tube heats or pyrolyzes the deposited solid particulate. Pyrolyzate vapors are generated, and they enter into a GC injector where a portion of the vapor enters the GC column module. Separation of the neutral vapors occurs, and the vapors elute into the IMS detector module. A 63-Ni ring ionizes the vapors, and the ions are pulsed in packets through a 4 cm drift region to a Faraday plate detector. The drift tube region has an applied electric field to guide the ions, and the entire IMS detector operates at close to atmospheric pressure. The bioaerosol detection event of the Py-GC-IMS contains further information in the GC-IMS dataspace.[21-23]

Bioaerosol discrimination was accomplished between deliberately released aerosols of Gram-positive Bacillus spores, Gram-negative bacteria, and ovalbumin (OV) protein because of their distinctive GC-IMS dataspace signatures.[23] In the present study, *Bacillus subtilis var. niger* (BG) and OV protein signatures were interrogated for their presence/absence over a 28-hr, continuous monitoring period of ambient bioaerosols in an urban environment near buildings at a work site. At random intervals, a spray pump application of biological substance was introduced near the inlet of the aerosol concentrator connected to the Py-GC-IMS. These series of experiments provided initial evidence that ambient background aerosols yield minimal to negligible interference in the daily, bioanalytical instrument monitoring of select target transient bioaerosol challenges.

2. EXPERIMENTATION

The Py-GC-IMS biodetector system was placed on a table platform in an urban area at the interface of a field and a forest (Figure 1). Work site buildings are located near the forest, and the biodetector was operated remotely inside the building. A 916-L/min XM-2 aerosol collector/concentrator (upper part of Figure 1, SCP Dynamics, Minneapolis, MN) was interfaced to the biodetector (lower section of Figure 1) by a Teflon-lined tube (TSI Inc., St. Paul, MN). The XM-2 has 50% and 26% efficiencies of aerosol collection for particulate with 5- and 2-μm diameters, respectively (unpublished data).

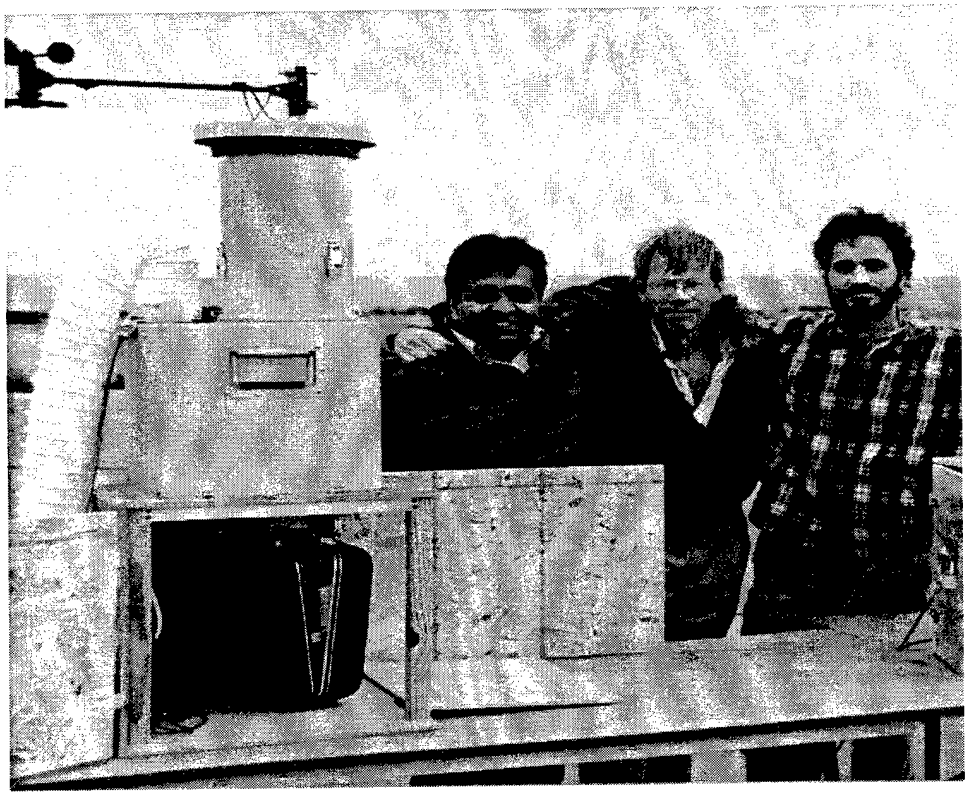

Figure 1. XM-2 Aerosol Concentrator Connected to the Py-GC-IMS Biodetector

An 8-channel Met One particle counter (Met One, Inc., Grants Pass, OR) was used to ascertain the total number of particles $\geq$0.5 μm diameter at 8 s intervals (11 s display time), and this provided independent information on the total particulate burden in the air. The particulate burden includes biological- and non-biological-containing particles.

The biodetector is housed inside a briefcase enclosure. The XM-2 is relatively larger (25 x 17 x 13 in.), heavier (approximately 66 lb), and uses more power (360 W) compared to the Py-GC-IMS (12 x 16 x 5 in., 15 lb including on-board computer, and a peak power at 120 W with a running power of 48 W). The experimental operating conditions and hardware parameters of the complete system can be found elsewhere.[21,23] Temperature measurements of the pyrolyzer, three-way injection valve, and GC were monitored with the use of type-K thermocouples connected to in-house-constructed electronic control boards.

Figure 2 shows the briefcase-size Py-GC-IMS. The main components are as follows: (1) aerosol inlet; (2) Pyrex tube/pyrolysis source; (3) vacuum pump interface to admit and deposit aerosol particulates onto the filter paper-quartz frit assembly; (4) high temperature three-way GC-injection valve; (5) patented,[29] programmable, ring-shaped GC column (high temperature, stainless-steel GC column, 4 m x 0.5 mm with 0.25 μm DB-1 methyl silicate coating, Quadrex Corporation, New Haven, CT); (6) 63-Ni ion source of the Chemical Agent Monitor (CAM) IMS (Smiths Detection, Bushey, Watford, Herts, WD23 2BW, UK); (7) dual diaphragm vacuum pump; (8) CAM ion mobility cell; (9) molecular sieve packs for scrubbing the ion mobility cell carrier gas; (10) molecular sieve packs to clean the ambient air; (11) 15 V DC power in; (12) Visionbook Traveler 3000 computer (Hitachi, Waltham, MA); (13) electronic hardware and power supplies underneath the computer; (14) 50-pin interface to PCMCIA data acquisition card; and (15) heavy duty briefcase.

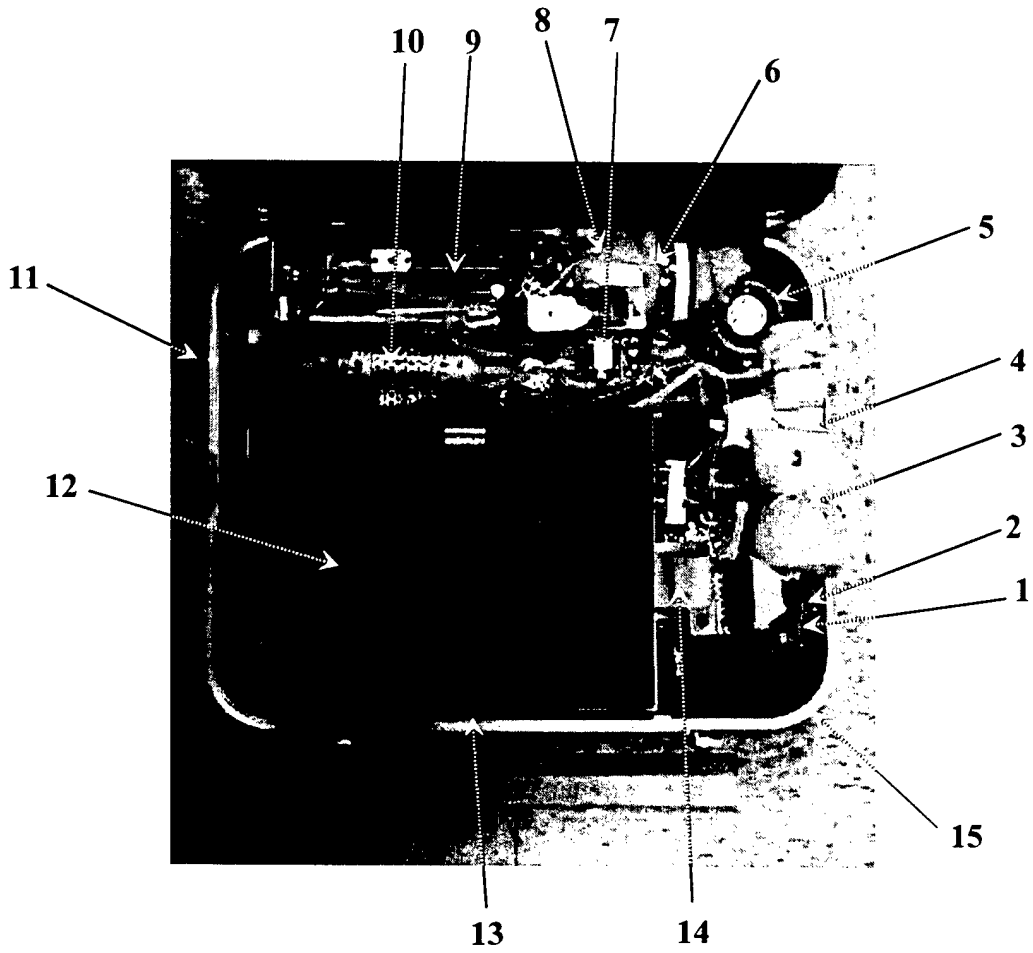

Figure 2. Briefcase Py-GC-IMS Biodetector

The four-stage XM-2 aerosol concentrator concentrated ambient aerosol particulates in the 2-10 μm diameter range. The pyrolysis source includes a quartz frit in the center of a Pyrex tube. A quartz micro fiber filter was placed on top of the frit, and this surface captured the aerosol particles from the fourth stage of the XM-2 with a minor flow of 500 mL/min from a downstream pump (#3, Figure 2). The aerosol particulate was dried, and with either pyrolysis or rapid heating at 350 °C, the pyrolyzate was generated from the collected aerosol particulate. A portion of the pyrolyzate vapor was admitted into the GC column. The eluate entered a 63-Ni ring ionization source at the entrance of the CAM IMS detector. Proton transfer, from protonated water molecule clusters, produces analyte ionization. A voltage gate pulses ions into a 4 cm drift tube at close to atmospheric pressure. The flight time of the ions through the atmospheric vapor molecules between the ion gate and the Faraday plate detector characterizes the ions. The IMS is essentially an atmospheric pressure time-of-flight detector. Due to the high pressure in the drift tube, ions are typically measured in millisecond drift times compared to the microsecond flight times of ions in a high vacuum time-of-flight instrument. The high IMS pressure also lowers the resolution of the ion mobility peaks to between 15-25. The molecular mass and cross-section are important factors in separating a mixture of ions in IMS.[30,31] Clean, dry air was used as carrier gas, and molecular sieve packs (#10, Figure 2) were used to scrub the ambient recirculation air.

A cycle of aerosol analysis begins with a 137 s collection of aerosol particulate (Figure 3) followed by a sample drying time with subsequent pyrolysis. The last 35 s of the previous cycle is also included in the total aerosol collection time. The collected particulate is dried for 16 s at 130 °C followed by pyrolysis at 350 °C. A 2.5-s injection of pyrolysis products enters the GC column, and analytical separation of the complex vapors ensues. Figure 3 shows a 40 s time period when the system is not collecting aerosol. The system is essentially blind to the environment during that time period. The aerosol collector is turned on again during the GC elution phase that occurs during the last 27 s of the cycle. This start of aerosol collection is a compromise between the collection of particulate into a relatively cool pyrolysis source and the reduction of "blind time" of the system to the environment. Approximately 3 min 3 s was currently used from the beginning of the cycle to GC elution and IMS detection of the biomarker compound. Depending on the GC retention time of the biomarker compound, this value varies with respect to the elution time (*vide infra*).

The computer in the Py-GC-IMS system was controlled at a distance of approximately 150 ft with wireless Ethernet antennae (Black Box Corporation, Lawrence, PA); PC ANYWHERE software (Symantec Corporation, Cupertino, CA); by a Dell Inspiron 3800 notebook computer (Dell, Round Rock, TX); via wireless Ethernet, and a 10 MBPS PCMCIA card (Linksys, Irvine, CA). A PCMCIA data acquisition DAQcard 1200 (National Instruments Corporation, Austin, TX) and in-house written software[19] were used to acquire GC-IMS data. The data stream was converted to an ASCII file. The ASCII file was post-processed with a Fortran program written in-house.

During the 3-week series of aerosol trials, the same GC column, pyrolysis tube, and molecular sieve packs were used. The pyrolysis quartz filters were replaced after every window of aerosol trials, and there were two windows per day. The filters experienced a buildup

of pyrolyzate char and tar in the form of gray-black deposits. No significant GC column degradation was noticed (i.e., no significant shift of analyte retention time), and the same air-scrubbing molecular sieve packages were used.

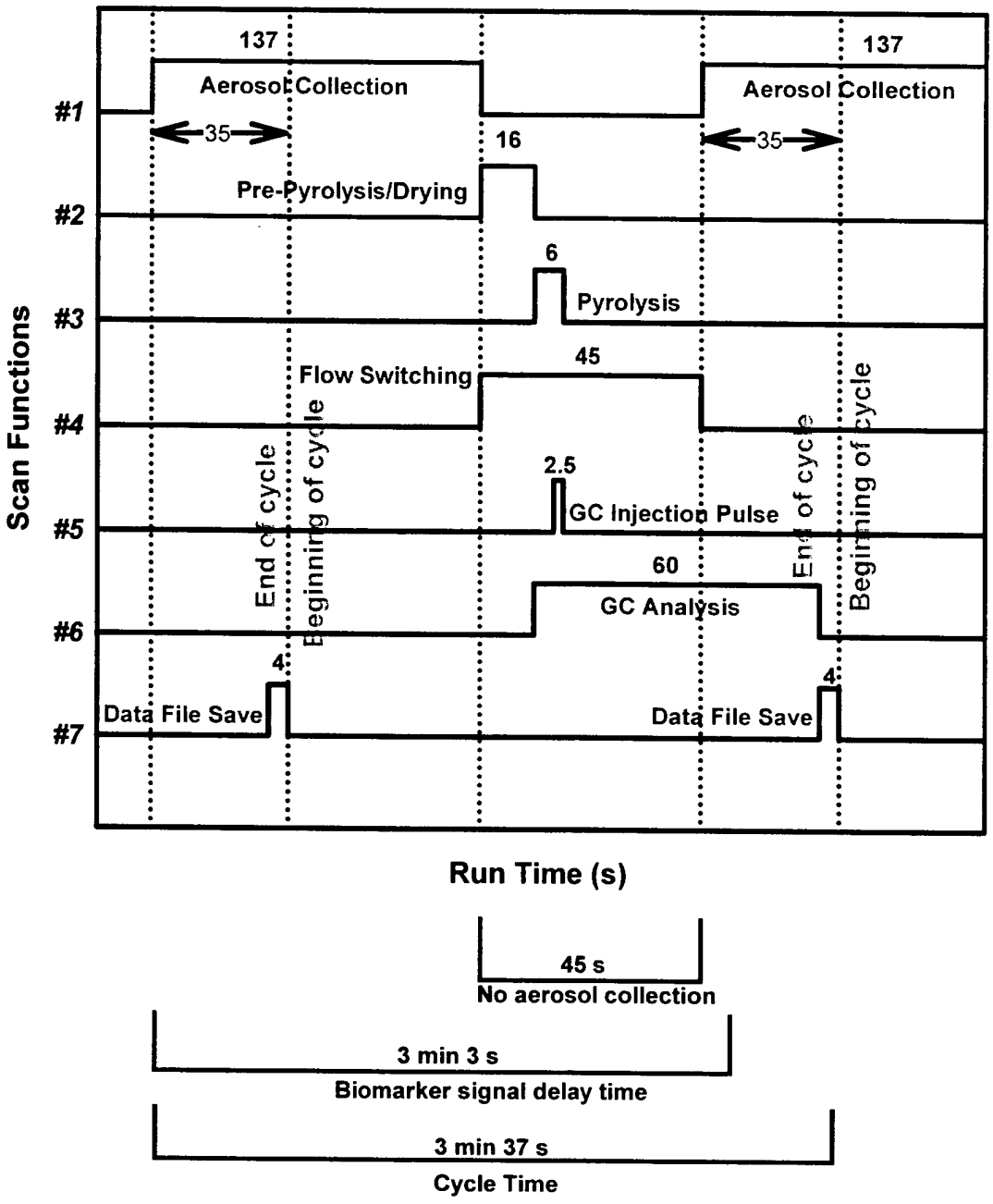

Figure 3. Outline Events and Timed Sequences in a Py-GC-IMS Analysis Cycle

From 2 March to 12 October 2001 each Friday morning to Saturday morning, the XM-2 – Py-GC-IMS system operated in a continuous fashion at the same outdoor location collecting, interrogating, and producing GC-IMS dataspaces every 3 min 37 s. The weather conditions and liquid/solid particulates (rain, fog, hot and cold temperatures) in the air varied considerably during these 8 months. During this time, the same GC column, pyrolysis tube, and molecular sieve packs were used. The pyrolysis filter paper was replaced at select intervals (*vide infra*) because the filters experienced a buildup of pyrolyzate char and tar in the form of gray-black deposits. No significant GC column degradation was noticed (i.e., no significant shift of analyte retention time), and the same air-scrubbing molecular sieve packs were used. At random intervals, a small-pressurized canister (BioPuffer) containing either dry BG spores or OV protein was pump activated approximately 0.5 m from the aerosol inlet of the XM-2. The inlet consists of a flat plate on top of the cylindrical aerosol concentrator as observed in Figure 1. The canister emits a metered, reproducible dose of biological particulate aerosol; however, an informal survey showed that a reproducible amount of bioaerosol does not enter into the XM-2 inlet. Amounts of BG spores in the BioPuffer canisters were 0.1%, 0.05%, and 0.01% by weight, and OV was present at 0.1% by weight. Surfactant chemicals and the propellant 1,1,1,2-tetrafluoroethane are also included in the canister. The surfactants facilitate the dispersion of the biological particulates.[38]

Multivariate data analysis was performed using SysStat version 10 (Systat Software, Incorporated, Richmond, CA) on the GC-IMS dataspace peak intensities. Raw data in the GC-IMS dataspace were divided into a grid, and each grid element represents an orthogonal dimension axis in multivariate data space. The intensities of the peaks in each grid element were integrated, and the resulting value was plotted on the respective orthogonal axis.

3. RESULTS AND DISCUSSION

The ambient aerosol background was interrogated about the site of the XM-2 – Py-GC-IMS analytical system. A complex mixture of biological, soot, inorganic, plant, and animal debris particulates can be found in an ambient urban outdoor aerosol. A major objective herein was to observe and analyze the response of a deliberately released, biological aerosol in the ambient environment of a complex outdoor urban aerosol from the GC-IMS dataspace generated from a Py-GC-IMS instrument.

3.1 Wide Area Dissemination of Bioaerosols in a Prairie.

Figure 4 contains the GC-IMS data displays of known OV and EH aerosols introduced into the XM-2 – Py-GC-IMS. The aerosols were disseminated from sprayers situated approximately 100-250 m from the Py-GC-IMS in a prairie environment. The GC dimension separates the complex pyrolyzate vapor mixture, and the IMS dimension separates the 63-Ni produced analyte ions by their size, shape, mass, and cross-section. The reactant ion peak (RIP) represents protonated water molecules. Water vapor continually elutes from the GC column. Through a series of ion-molecule reactions, molecular nitrogen becomes ionized in the 63-Ni region and ultimately produces protonated water molecules. The hydrogen bond between the proton and water molecules is relatively weak, and the proton is usually transferred to a neutral

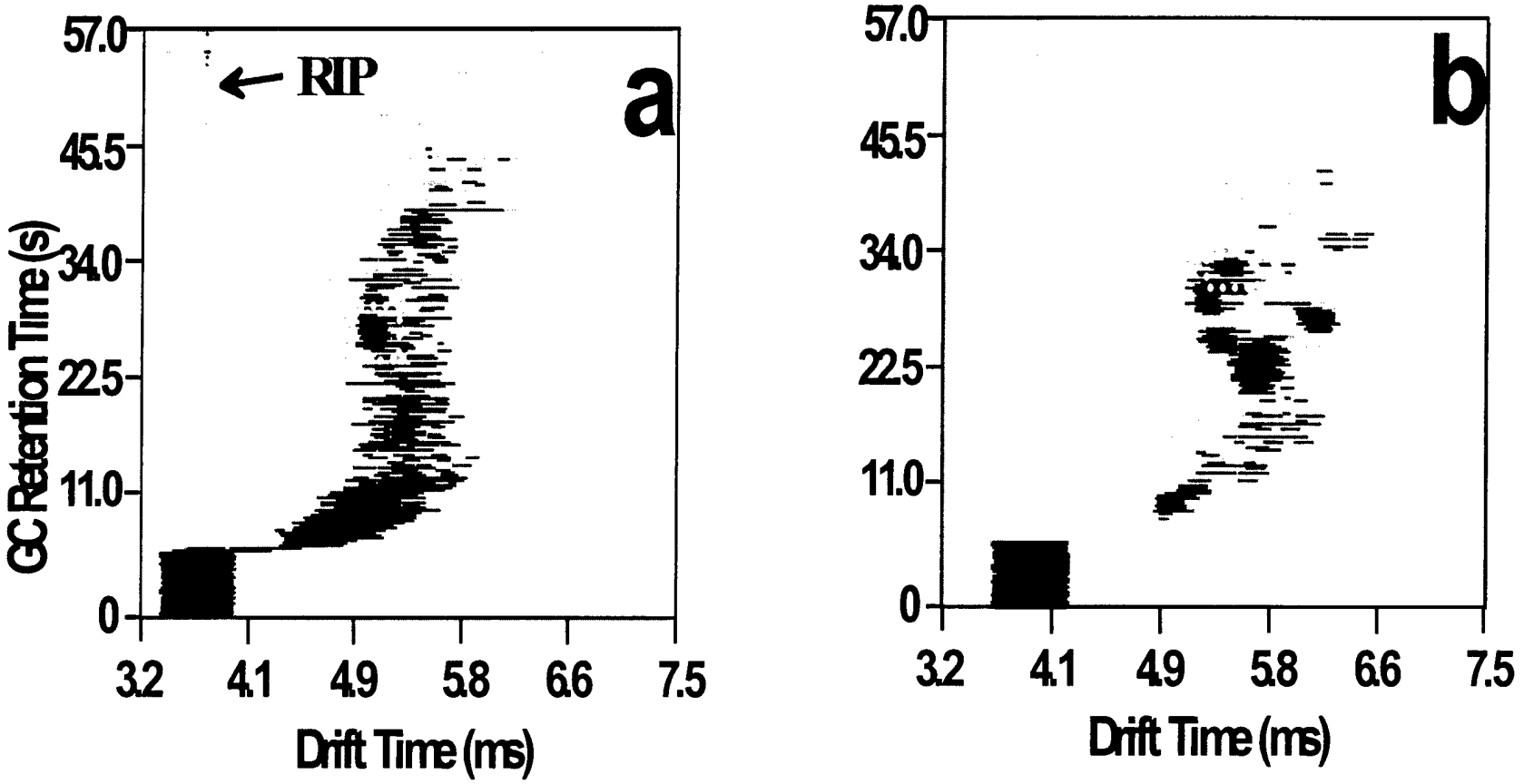

Figure 4. GC-IMS Data Domains of the Following Known Aerosols Released 100-250 m from the Biodetection Systems. (a) EH bacteria, (b) OV. Dotted boxes depict the specific biomarker compounds used in a visual analysis for the presence/absence of a biological substance in aerosol trials.

analyte molecule having an organic functional group containing sulfur, nitrogen, or oxygen. In the absence of analyte, only the RIP is present, signifying a continual presence of protonated water molecules. When a sample is present, protons are transferred, the RIP intensity is reduced, and a new peak is present at a longer drift time. Higher concentrations of analyte result in a reduced to absent RIP signal intensity.

It is instructive to show a known bioaerosol episode and respective response of the Py-GC-IMS in a low aerosol particle burden per liter of background air in an outdoor environment. Background aerosols are very low in a prairie environment (50-200 particles per liter of air) and thus provide a very low interference for bioanalyte aerosols.[23] For the prairie environment during the August-September 2000 outdoor bioaerosol tests, a two-channel Met One registered the following information on particle size in microns and average number of particles per liter of air: 0.5, 643; 1.0, 156. This enables an appreciation and comparison to GC-IMS events in an urban setting where the background aerosol burden is significantly higher (*vide infra*) than the prairie environment. Figure 4a shows a complex GC-IMS pyrolyzate pattern for EH. The dotted box outlines a peak that is relatively distinct for EH, and Figure 4b shows that of OV. The dotted boxes in Figures 4a,b outline GC-IMS dataspace locations that were used in a qualitative analysis and differentiation for the presence for each of the bioaerosols.[23] These selected locations in GC-IMS dataspace were treated as biomarkers and used to interrogate for the presence of EH- and OV-related signals in a daylong record of the GC-IMS dataspace collection of ambient aerosols.

Figure 5 shows a series of GC-IMS responses from the pyrolyzate GC separation of an aerosol dissemination of BG spores.[23] Note the presence of a RIP peak in some of the GC-IMS dataspaces as well as differential signal displays. The dotted boxes delineate specific locations where peaks are evident in the GC-IMS dataspace. These peaks have been shown to represent the picolinic acid species.[33] Gram-positive spores contain 5-15% calcium dipicolinate,[34] and a pyrolysis product of the dipicolinic acid organic chelate is picolinic acid.[33] This compound has a high proton affinity, and it occupies relatively distinct places in GC-IMS dataspace. The series of GC-IMS dataspaces (Figures 5a-i) represent responses of an aerosol release of BG spores over a period of time. Each of the nine plotted points in Figure 5j represent the summation of the total ion current (TIC) bounded in the (x,y) GC-IMS region (IMS drift time in milliseconds, GC retention time in seconds) as follows: 4.2, 5.0 ; 9.0, 5.0; 4.2, 15.0; 9.0, 15.0. The points in Figure 5j represent Figures 5a-i in successive time intervals. The point at 17:00:47 represents the integrated TIC value for Figure 5a, etc. Note the increased total intensity at 17:06:51, and its spectral representation is shown in Figure 5c. A relatively similar intensity is observed for the fourth point, and the fifth point (Figure 5e) approaches background levels compared to Figure 5a. The sixth point increases considerably in signal strength, and a complex pyrolyzate pattern is observed in Figure 5f. The seventh and eighth data points at 17:18:58 and 17:22:01, respectively, indicate continued complex signals for the BG aerosol (Figures 5g,h). The last plotted point (representing Figure 5i) in Figure 5j corresponds to background signal. Note the relatively rapid departure of the BG aerosol from Figure 5h to 5i. This is characterized by a virtual complete absence of a RIP (Figure 5h) to a prominent RIP signal (Figure 5i). The duration of the BG cloud about the instrument detector was about 21 min.

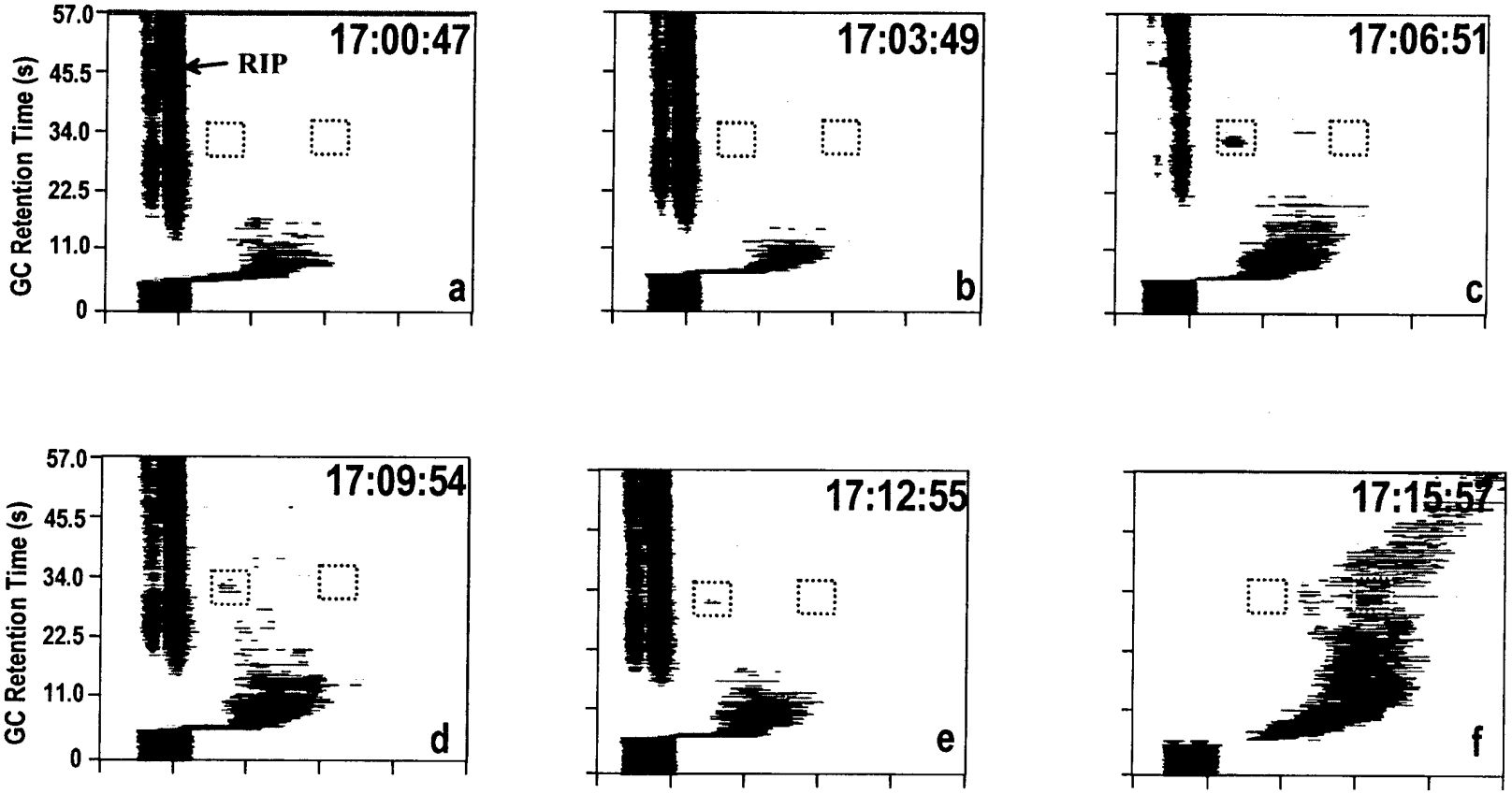

Figure 5. (a-i) Consecutive GC-IMS Dataspaces of a BG Aerosol Event Released 100-250 m from the Biodetection System. (j) Total activity or total ion current plot of each GC-IMS dataspace. Each point represents integrated intensities in the respective GC-IMS dataspace as shown in (a-i). (k) Selected peak area plots of three bioaerosols. Intensities in the dotted boxes in (a-i) were integrated and plotted as BG (o). The location of the dotted boxes in Figures 4a, b were applied to (a-i), and signals in the boxes were integrated and plotted as EH (Δ) and OV (□).

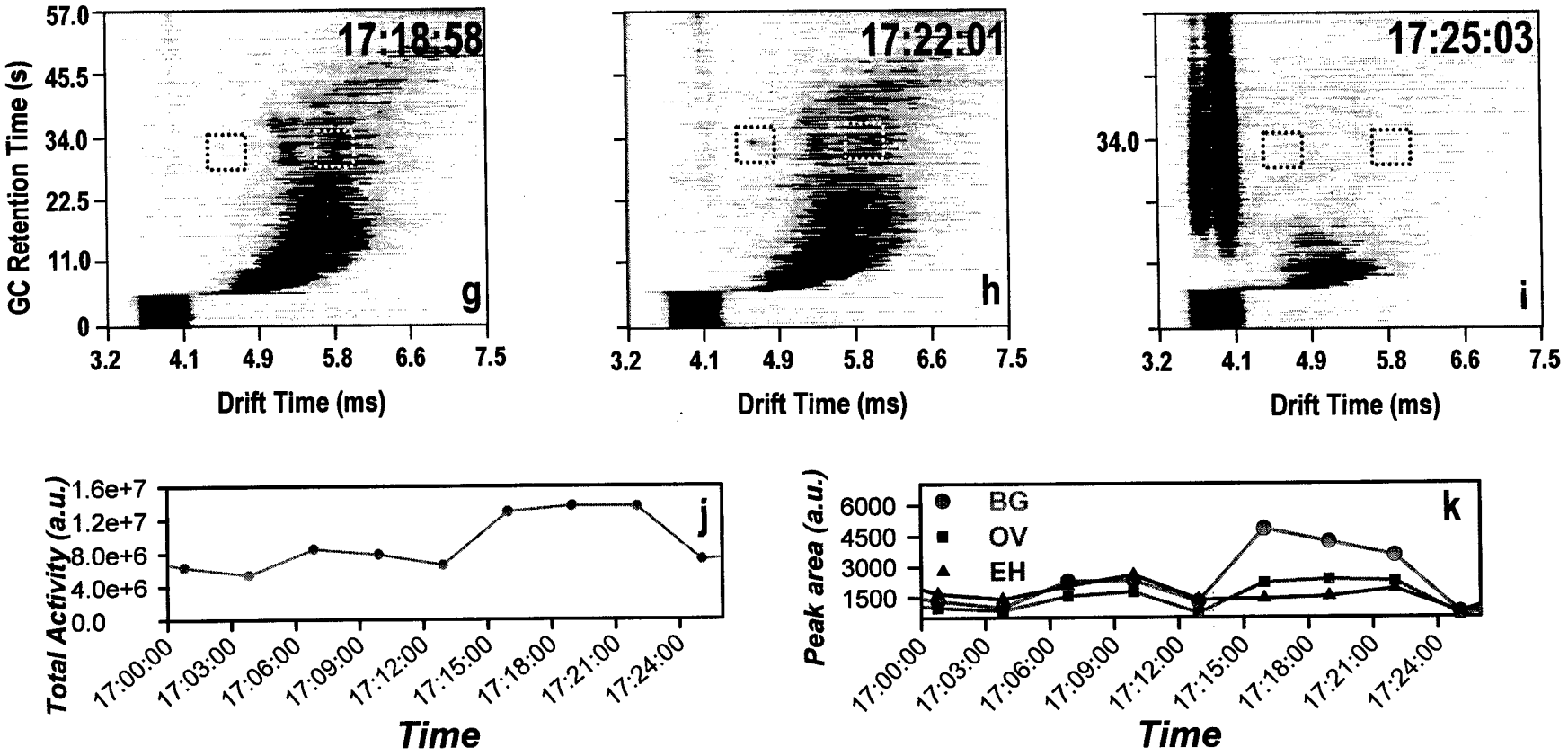

Figure 5 (Continued). (a-i) Consecutive GC-IMS Dataspaces of a BG Aerosol Event Released 100-250 m from the Biodetection System. (j) Total activity or total ion current plot of each GC-IMS dataspace. Each point represents integrated intensities in the respective GC-IMS dataspace as shown in (a-i). (k) Selected peak area plots of three bioaerosols. Intensities in the dotted boxes in (a-i) were integrated and plotted as BG (o). The location of the dotted boxes in Figures 4a, b were applied to (a-i), and signals in the boxes were integrated and plotted as EH (Δ) and OV (□).

Figure 5k tracks only the integrated intensity in the dotted boxes in GC-IMS dataspace in Figure 4 for EH and OV and Figures 5a-i for BG. The BG peak area plot (circles) in Figure 5k provides a similar plot to that of the TIC in Figure 5j. Figure 4a shows one distinct biomarker location in GC-IMS dataspace for EH characterization, and Figure 4b presents two biomarker locations for OV. Figure 5 shows two biomarker locations for BG discrimination. Thus, there are five distinct regions in GC-IMS dataspace for the differentiation of BG, EH, and OV bioaerosols.

3.2 Discrete Bioaerosol Dissemination in an Urban Environment.

Figure 6 displays aerosol particulate information from a Py-GC-IMS monitoring of an ambient, urban outdoor atmosphere in the 11-12 October 2001 timeframe. An eight-channel Met One particle counter registered the following information in terms of particle size in microns and average particles per liter of air: 0.5, 2047; 1, 675; 2, 261; 3, 69; 4, 27.

Figure 6a shows the total GC-IMS signal intensity of the atmospheric particulate burden as registered by the Py-GC-IMS. Each point is the result of one GC-IMS dataspace, and a point represents a summation (TIC) of all the intensities of peaks above a certain threshold contained in the area bounded by the following four millisecond, second locations in GC-IMS dataspace: 4.8, 10.0; 9.0, 10.0; 4.8, 45.0; 9.0, 45.0. These urban-derived values are different than those from the prairie environment (*vide supra*) because the atmospheric pressure is significantly different between the locales. Pressure directly affects the drift time of ions in the IMS drift tube cell.

There are four vertical dotted lines in Figure 6, and they represent the times when the filter paper was replaced in the pyrolysis Pyrex tube. The baseline response of the 25 GC-IMS dataspaces centered about 23:00:00 is due to an electronics failure in the circuit board that processes the IMS ion current. The dotted box locations in the GC-IMS dataspaces in Figures 4 and 5 (depicted as TIC points) were scanned over all 477 dataspaces in Figure 6a. The integration values of signals in all five dotted box locations (Figures 4 and 5) for each dataspace are plotted as individual curves in Figure 6b. Note that in Figure 6a, a dynamic response is generally observed where the total signal activity fluctuates significantly over the 28-hr interrogation timeframe. Figure 6b shows a relatively consistent low-intensity baseline with a number of "spikes." In Figure 6b, the peak area plots of the five separate dotted box locations in Figures 4 and 5 are orders of magnitude lower than the summation (TIC) of the entire GC-IMS dataspace signals (Figure 6a).

The BG, EH, and OV are represented in Figure 6b as the symbols o, Δ, and □, respectively. Select regions in Figure 6b are highlighted as letters a-d and f-i. These places in the 28-hr investigation represent BioPuffer sprays of the following: 0.1% BG at points a, b, c, f; 0.05% BG at point g; 0.01% BG at point d; 0.1% OV at points h and i. Point e in Figure 6b represents either a blank or no deliberate BioPuffer spray, and point j represents a spray of TiO_2 particles.

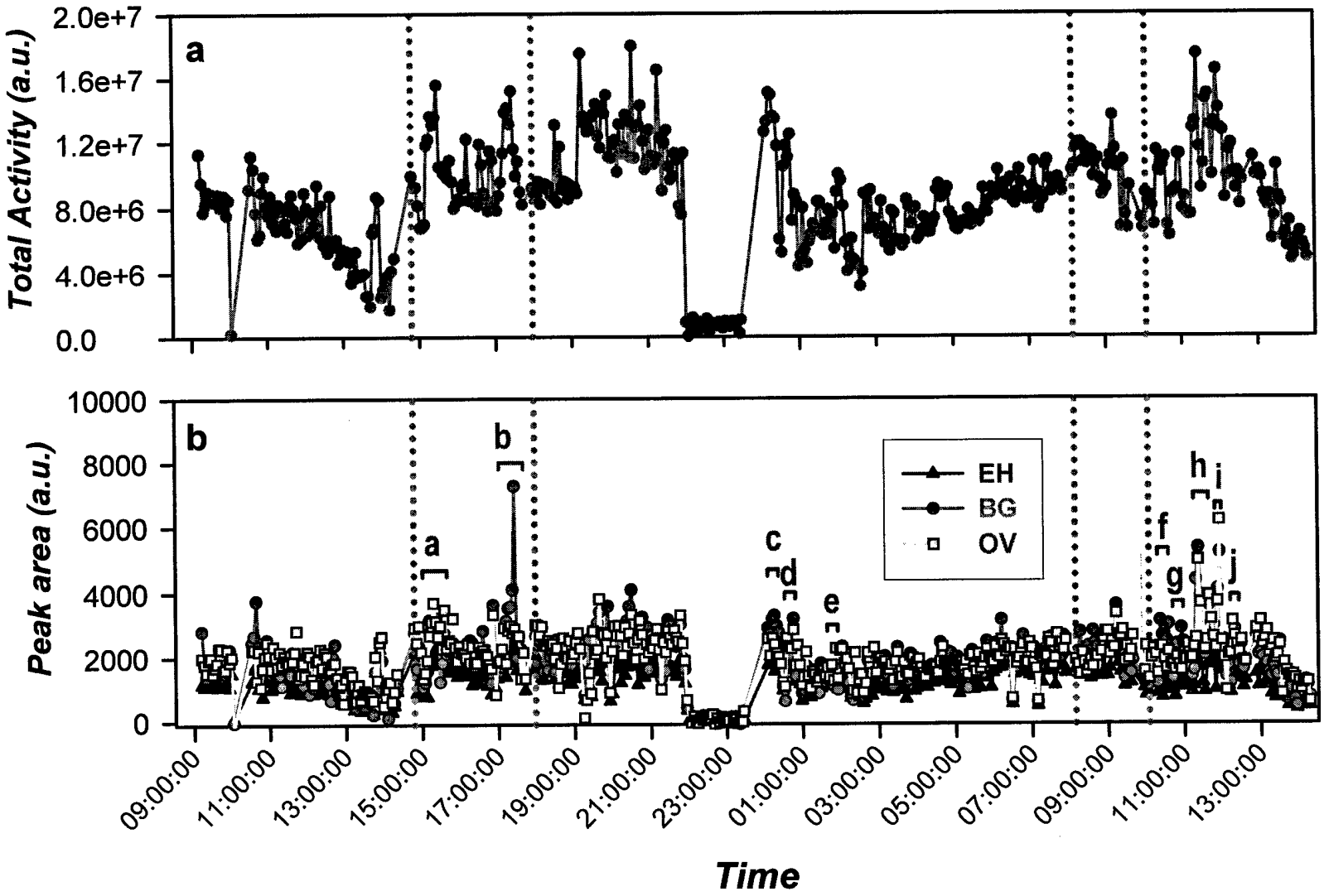

Figure 6. Consecutive 3 min 37 s GC-IMS Integrated Intensity Plots of (a) Total Ion Current and (b) Selected GC-IMS Biomarker Peak Areas for the 11-12 October 2001 Atmospheric Aerosol Background Monitoring with Selected Bioaerosol Releases Near the Biodetection System

Figure 7 presents individual GC-IMS dataspaces with the time label as to its location in Figure 6b. Note that there is a general absence of sample species in the majority of the dataspaces. A strong, well-defined RIP is observed for each dataspace. The discontinuity in each RIP represents the pyrolysis event, and the species eluting from the GC originate from the pyrolyzed particulates. These species represent light-in-mass gases because they have short retention times and fast ion drift times (relatively high ion mobility values). The two lower graphs in Figure 7 represent a magnified view of region e in Figure 6 and are analogous to that of Figures 5j,k. Both graphs at the bottom of Figure 7 are relatively featureless with respect to the presence of an aerosol event.

The majority of the "spikes" above the general baseline in Figure 6b represent BioPuffer BG sprays. There is an OV-related event at approximately 14:00:00. No OV was either sprayed or tested at this time, and the appearance of the signal is at a relatively low level. The overall EH signal in Figure 6b essentially tracks in the background level, and EH was neither sprayed nor tested in this 28-hr test window. There is a significant OV event near the end of the window in the 11:55:35 region (points h and i in Figure 6b). The OV protein signatures were observed above the general background (data not shown) with respect to the GC-IMS biomarker areas indicated in Figure 4b. This is the only time that OV was sprayed during the 28-hr timeframe. A few relatively low intensity OV peaks are observed in the first half of Figure 6b. In general, the highlighted OV peaks in Figure 4b can generally be found in the low level background in Figure 6b except for the deliberately sprayed timeframe about 11:55:35.

The two upper graphs in Figure 8 present a magnified view of region b in Figure 6b. An aerosol of BG spores was released at that time, and a clear event is observed above the general background. Twelve GC-IMS dataspaces are presented that comprise region b in Figure 6b. Each GC-IMS dataspace is depicted sequentially by time, and the first three dataspaces represent background. A RIP is present in these three dataspaces and very little signal is observed in later GC retention times with respect to the initial light gases that evolve from the pyrolysis event. Two dotted boxes are depicted in each GC-IMS dataspace, and they represent the places where the picolinic acid signatures are observed in the standard BG aerosol data in Figure 5. The signals in the dotted boxes in the first three GC-IMS dataspaces are relatively low in intensity. The next five dataspaces essentially show a complete depletion of the RIP and relatively complex signals. Intensities in the dotted boxes, especially at 17:18:57, 17:22:20, and 17:25:37 provide signals indicative of the presence of picolinic acid. Maximum BG presence occurs at 17:25:37, and this is summarized in the upper right hand peak area (TIC) plot in Figure 8. The wide band of signals in each GC-IMS dataspace from 17:12:16 to 17:25:37 shows a trend that later eluting pyrolyzate products occur at longer drift times. This can be rationalized that as the molecular weight of a substance increases, the longer the GC retention time and the slower the ion drift time in the IMS electric field near atmospheric pressure.

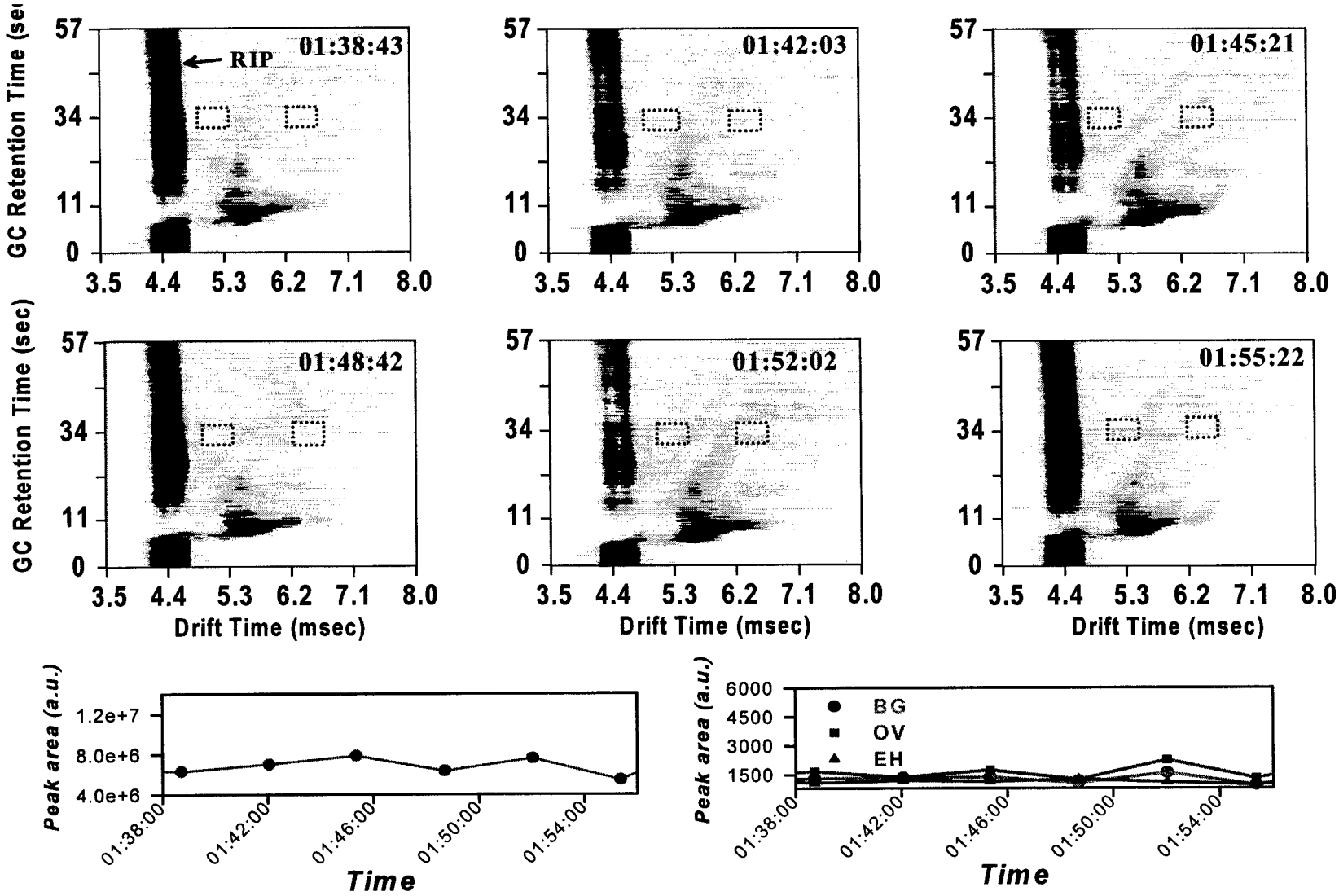

Figure 7. Consecutive GC-IMS Dataspaces in the 01:38:43-01:55:22 Time Regions in Figure 6 Where a Release of Bioaerosol was not Performed. Bottom two traces are analogous to Figure 5j, k

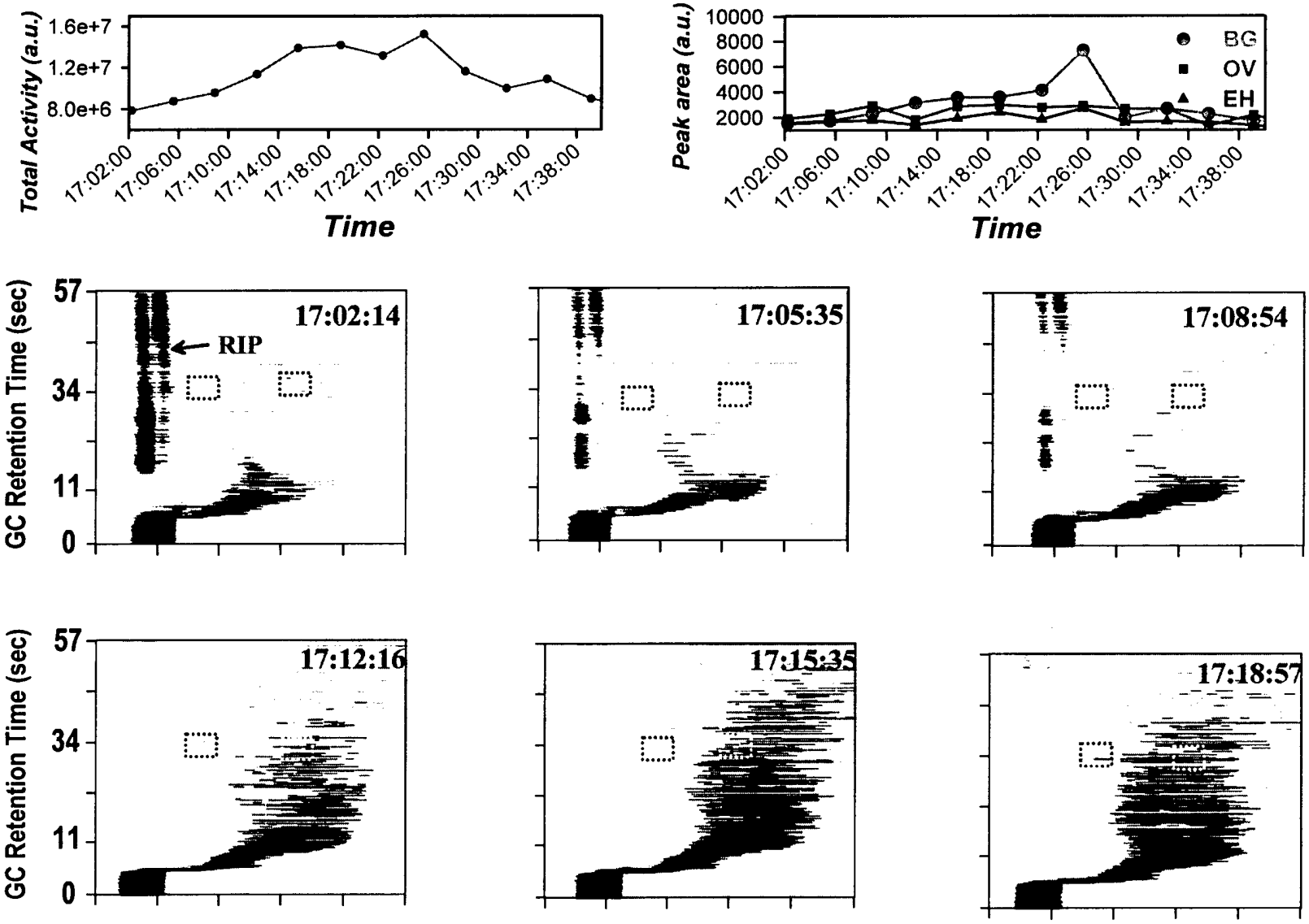

Figure 8. Series of 12 GC-IMS Dataspaces that Highlight a BG Aerosol Release from Figure 6

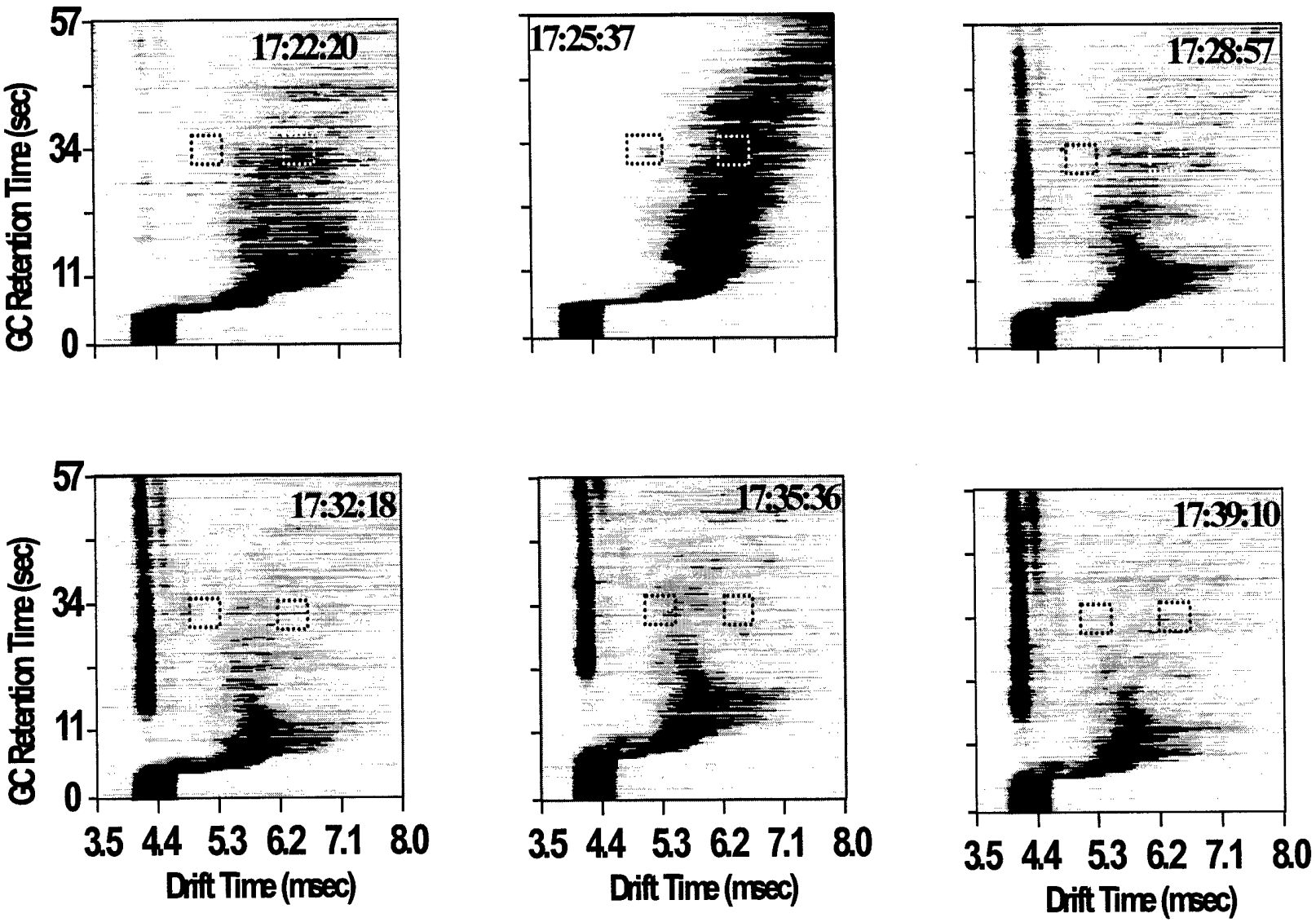

Figure 8. Series of 12 GC-IMS Dataspaces that Highlight a BG Aerosol Release from Figure 6 (Continued)

The last four dataspaces show a return of the RIP and a significant reduction in picolinic acid signal strength in the dotted boxes. Note the decrease of signal strength in the two dotted boxes in each of the last four dataspaces compared to the previous five GC-IMS dataspaces. In addition, the overall trend and patterns of signals in the GC-IMS dataspaces in Figure 8 are analogous to the eight GC-IMS dataspaces from the BG aerosol standard in Figure 5. The other BG events noted in Figure 6b follow similar patterns of signals as those of event b in Figure 6b.

This analysis is relatively straightforward in concept and relies on a visual characterization of the data; however, it has been very useful in distinguishing BG, EH, and OV aerosols under extensive outdoor field trials.[18]

3.3 Statistical Analysis of the Bioaerosol Events.

An unbiased, sophisticated data analysis was used on the complex dataset, and it consisted of multivariate analysis statistics.[35, 36] Figure 9 shows five "shotgun" factor plots of all 477 GC-IMS dataspaces in the 28-hr experimental window (Figure 6).

Figure 9a presents a factor 1-2 plot of the 477 GC-IMS dataspaces plotted in Figure 6. Most of the points represent low total ion current background and are represented as sequential numbers in time with respect to Figure 6. The GC-IMS dataspaces that show signatures for BG, OV, and inert TiO_2 are plotted as o, □, and Δ, respectively. Open BG circles represent lower bioaerosol concentrations, and filled circles represent relatively higher BG aerosol concentrations about the aerosol concentrator. Note that the lower BG concentration points (open circles) lie nearer to the factor plot origin than the filled circles, higher BG bioaerosol concentrations. This is due to the relatively lower integrated signals referenced in Figure 5. The 25 points centered about 23:00:00 in Figure 6 are represented in Figure 9 as a cluster at the factor 1-2 coordinates of –2.5, 2.2.

In each plot in Figures 9a-e, a region was manually drawn that placed a boundary around selected sets of biological and inert TiO_2 aerosol symbols. The background numbers residing outside of the boundaries in region 2 (Figure 9a), region 4 (Figure 9b), region 6 (Figure 9c), and region 11 (Figure 9e) were removed. This procedure resulted in only six remaining background-containing GC-IMS dataspace points in the plots. Therefore, multivariate factor analysis appears to be useful for continuous, repetitive analytical datasets with respect to filtering and separating biological from nonbiological aerosol events. Figures 10a-e magnify the results of the background filter exercise in Figure 9. A clear analysis emerges from the filter techniques for distinguishing the bioaerosols in Figure 10. The factor 1-2 plot concentrates the bioaerosols into one region with no obvious separation. The factor 1-3 plot provides a somewhat similar analysis to the factor 1-2 plot except that the inert TiO_2 aerosol event is relatively more separated in Figure 10b than the event is in Figure 10a. Figure 10c shows that a factor 1-5 plot presents separation tendencies between the BG and OV aerosols, and the lower concentration BG aerosol (open circles) tends to cluster about the factor origin. Figure 10d (factor 2-5 plot) clearly separates OV from BG and TiO_2, and Figure 10e (factor 3-5 plot) resolves the BG and OV biological and TiO_2 nonbiological aerosol events.

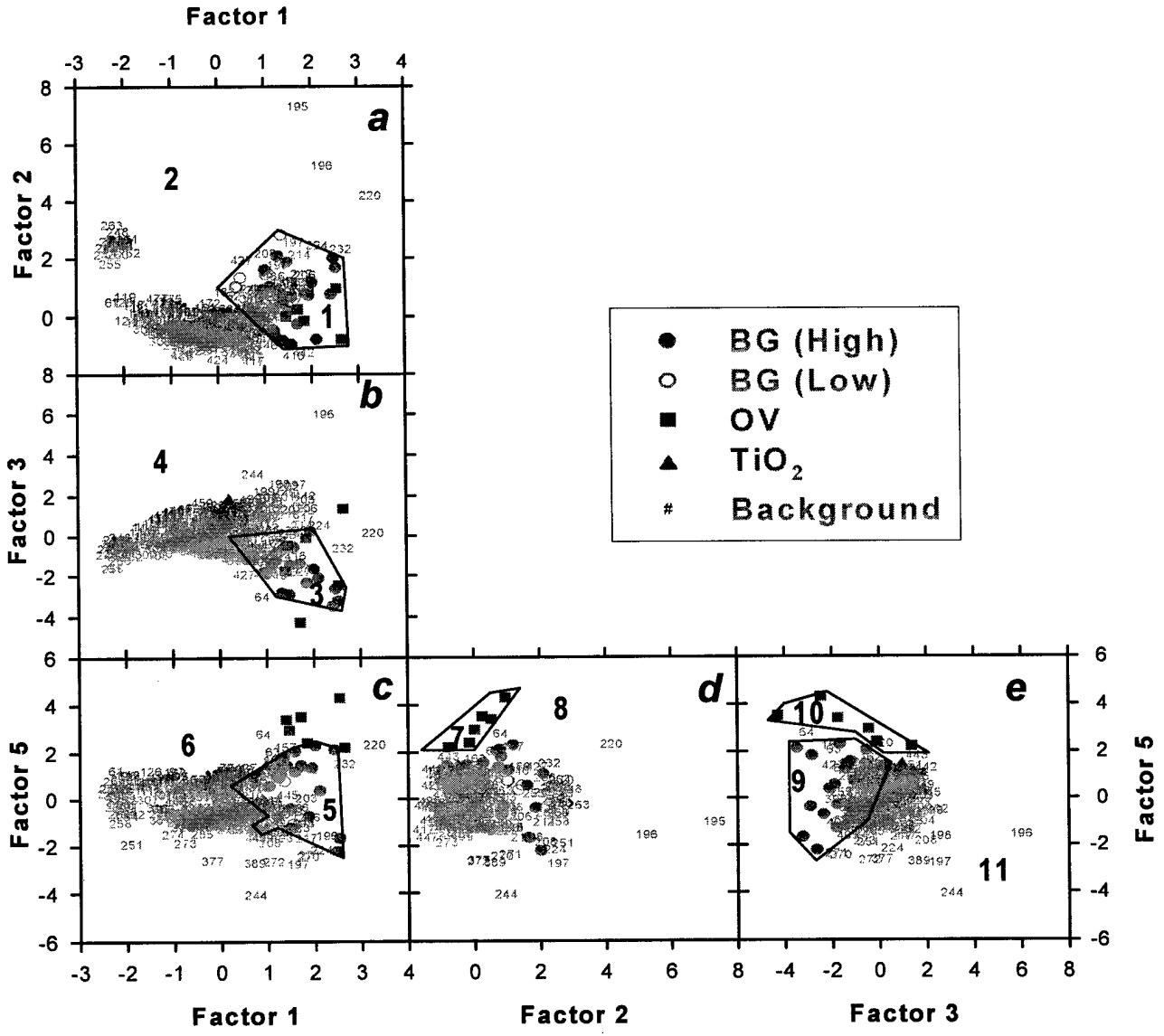

Figure 9. Five Multivariate Factor Dataspaces that Present a Unified Statistical View of all 477 Individual GC-IMS Cycles from Figure 6

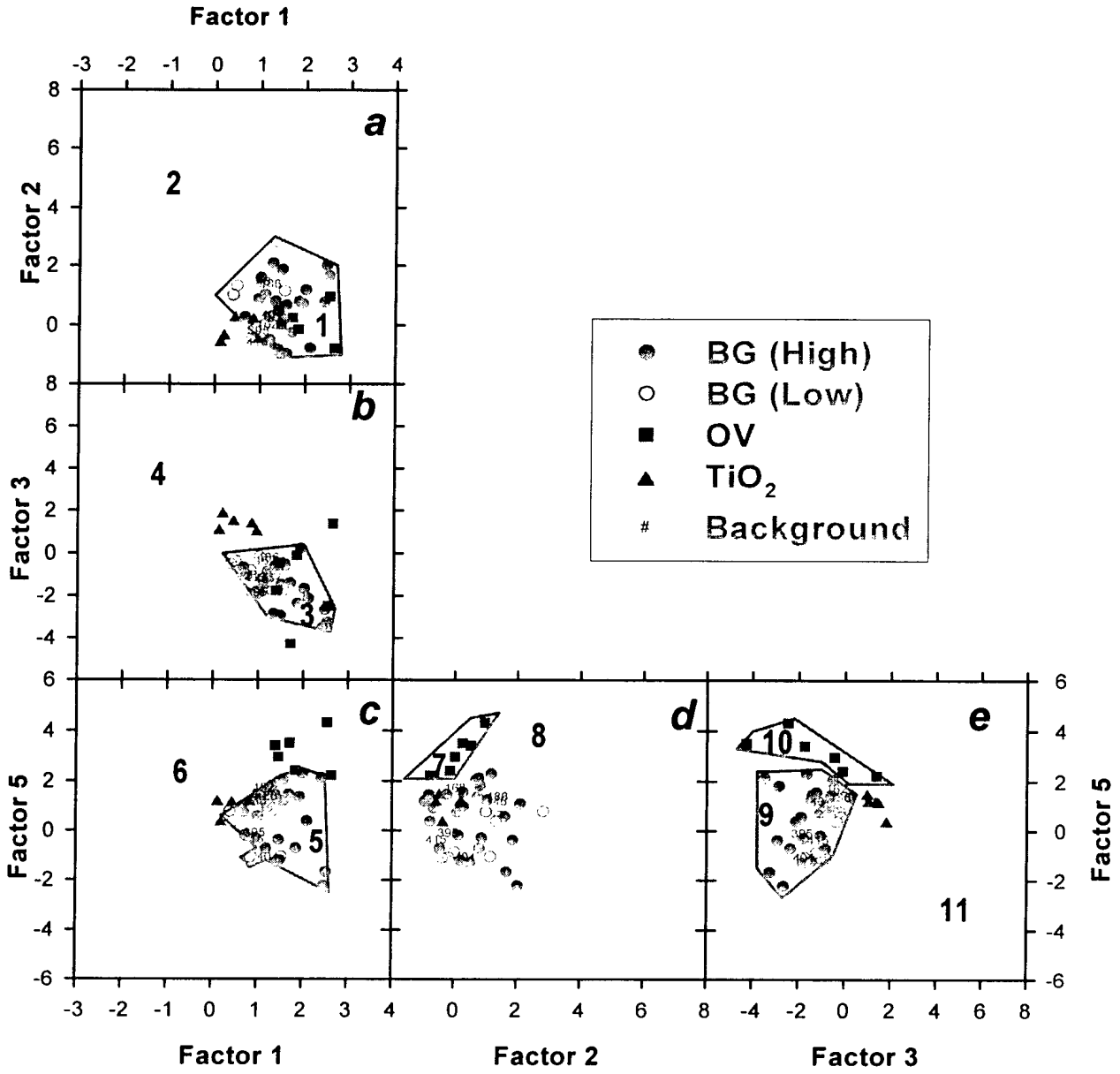

Figure 10. Five Multivariate Dataspaces from Figure 9 After Filtering out the Background, Non-bioanalyte Containing, GC-IMS Cycles

This analysis produces a set of guidelines for delineating the presence of a certain bioaerosol in Figure 10. The GC-IMS dataspaces containing BG aerosol signatures should be represented in zones 1, 3, 5, 8, and 9, and BG should not be present in zones 2, 4, 6, 7, 10, and 11. The OV aerosol should be present in zones 1, 6, 7, and 10 and should not be found in zones 2, 5, 8, 9, and 11. The filtering procedures performed in Figure 9 removed background-containing dataspaces from zones 2, 4, 6, and 11. After this filtering procedure, background aerosol points should not be present in zone 7 and should be absent in at least one of zones 1, 3, 5, 9, and 10. It is observed that the few remaining background signature-containing GC-IMS dataspaces are found in zones 1, 3, 5, 8, and 9, and are absent in zones 7 and 10.

4. CONCLUSIONS

In the environment, in general, isolated, short temporal episodes of biological aerosol releases are observed rarely. Rather, continuous mechanisms of release of biological material occur. This generates short and long term patterns of bioaerosol presence that are associated with the atmospheric aerosol burden.[4, 5, 8, 9, 13, 17] The pyrolysis-gas chromatography-ion mobility spectrometry (Py-GC-IMS) bioanalytical system was used to interrogate short bursts of bioaerosols. The biological substances were deliberately aerosolized into the ambient atmosphere near the entrance of the aerosol collector; a degree of mixing and dilution of the biological aerosol occurred within the background aerosol prior to introduction into the aerosol collector. The aerosol collector concentrated a relatively high ambient background particulate burden along with a relatively low amount of released biological spray. However, the respective biological substance signals were observed visually and delineated by the data reduction and analysis software. The bioanalytical system analysis of the atmosphere occurred in repetitive, relatively short 3 min 37 s interrogation cycles.

No attempt was made to investigate the biological constitution of the ambient background atmospheric aerosol with either bioanalytical or classical microbiology methods. The complex ambient background aerosol was processed by the bioanalytical system into sequential GC-IMS dataspace cycles. The response set from each GC-IMS dataspace was then reduced to a single point in multivariate space.

The observation of bioaerosol presence in a 28-hr window by deliberate, brief biological substance releases into an aerosol sampling system with continuous bioanalytical detection attempts to address biological aerosol monitoring concerns in ambient atmospheric analysis. An aerosol concentrator connected to a Py-GC-IMS continuous detection system has shown capabilities to provide biological event detection at discrete times spanning relatively narrow time intervals. In addition, biological classification information was produced upon statistical analysis reduction of the GC-IMS data. In general, the relatively high, urban atmospheric aerosol particulate burden provided minimal-to-negligible interference in the interrogation of presence and type of short bursts of bioaerosols by a Py-GC-IMS biological detection system.

Blank

LITERATURE CITED

1. DeCosomo, G.A.L.; Griffiths, W.D. Problems Associated with the Assessment of Airborne Microorganisms. *J. Aerosol Sci.* **1992,** 23, Suppl. 1, pp S655-S658.

2. DeCosomo, G.A.L.; Stewart, I.W.; Griffiths, W.D.; Deans, J.S. The Assessment of Airborne Microorganisms. *J. Aerosol Sci.* **1992**, 23, Suppl. 1, pp S683-S686.

3. Griffiths, W.D.; DeCosomo, G.A.L. The Assessment of Bioaerosols: A Critical Review. *J. Aerosol Sci.* **1994**, 25, pp 1425-1458.

4. Lighthart, B. The Ecology of Bacteria in the Alfresco Atmosphere. *FEMS Microb. Ecol.* **1997**, 23, pp 263-274.

5. Jensen, P.A.; Lighthart, B.; Mohr, A.J.; Shaffer, B.T. Instrumentation Used with Microbial Aerosols. In *Atmospheric Microbial Aerosols: Theory and Applications*; Lighthart, B., Mohr, A.J., Eds., Chapter 8; Chapman and Hall, Inc.: New York, 1994; pp 226-284.

6. Spurny, K.R. Chemical Analysis of Bioaerosols. In *Bioaerosols Handbook*; Cox, C.S., Wathes, C.M., Eds., Chapter 12; CRC Press, Inc., Lewis Publishers: Boca Raton, FL, 1995; pp 317-334.

7. Jones, B.L.; Cookson, J.T. Natural Atmospheric Microbial Conditions in a Typical Suburban Area. *Appl. Environ. Microbiol.* **1983**, 45, pp 919-934.

8. Shaffer, B.T.; Lighthart, B. Survey of Culturable Airborne Bacteria at Four Diverse Locations in Oregon: Urban, Rural, Forest, and Coastal. *Microb. Ecol.* **1997**, 34, pp 167-177.

9. Lighthart, B.; Shaffer, B.T. Airborne Bacteria in the Atmospheric Surface Layer: Temporal Distribution Above a Grass Seed Field. *Appl. Environ. Ecol.* **1995**, 61, pp 1492-1496.

10. Lighthart, B.; Shaffer, B.T. Bacterial Flux from Chaparral into the Atmosphere in Mid-Summer at a High Desert Location. *Atmos. Environ.* **1994**, 28, pp 1267-1274.

11. Mancinelli, R.L.; Shulls, W.A. Airborne Bacteria in an Urban Environment. *Appl. Environ. Microbiol.* **1978**, 35, pp 1095-1101.

12. Bovallius, A.; Bucht, B.; Roffey, R.; Ana, P. Three-Year Investigation of the Natural Airborne Bacterial Flora at Four Localities in Sweden. *Appl. Environ. Microbiol.* **1978**, 35, pp 847-852.

13. Kelly, C.D.; Pady, S.M. Microbiological Studies of Air Masses Over Montreal During 1950 and 1951. *Canadian J. Botany* **1954**, 32, pp 591-600.

14. Prospero, J.M.; Blades, E.; Mathison, G.; Naidu, R.; Ginoux, P. *Interhemispheric Transport of Viable Fungi and Bacteria with Dust from Africa to the Caribbean: Sources and Transport Patterns*. Presented at the 15th Conference Biometeorology/Aerobiology and 16th International Congress Biometeorology, Kansas City, MO, 2002; paper 13A.3.

15. Hjelmroos, M. Relationship Between Airborne Fungal Spore Presence and Weather Variables. *Grana* **1993**, 32, pp 40-47.

16. Seaver, M.; Eversole, J.D.; Hardgrove, J.J.; Cary, W.K. Jr.; Roselle, D.C. Size and Fluorescence Measurements for Field Detection of Biological Aerosols. *Aerosol. Sci. Technol.* **1999**, 30, pp 174-185.

17. Reyes, F.L.; Jeys, T.H.; Newbury, N.R.; Primmerman, C.A.; Rowe, G.S.; Sanchez, A. Bio-Aerosol Fluorescence Sensor. *Field Anal. Chem. Technol.* **1999**, 3, pp 240-248.

18. Luoma. G.A.; Cherrier, P.P.; Retfalvi, L.A. Real-Time Warning of Biological-Agent Attacks with the Canadian Integrated Biochemical Agent Detection System II (CIBADS II). *Field Anal. Chem. Technol.* **1999**, 3, pp 260-273.

19. Ho, J.; Spence, M.; Hairston, P. Measurement of Biological Aerosol with a Fluorescent Aerodynamic Particle Sizer (FLAPS): Correlation of Optical Data with Biological Data. *Aerobiologia* **1999**, 15, pp 281-291.

20. Eversole, J.D.; Cary, W.K. Jr.; Scotto, C.S.; Pierson, R.; Spence, M.; Campillo, A.J. Continuous Bioaerosol Monitoring Using UV Excitation Fluorescence: Outdoor Test Results. *Field Anal. Chem. Technol.* **2001**, 5, pp 206-212.

21. Snyder, A.P.; Maswadeh, W.M.; Parsons, J.A.; Tripathi, A.; Meuzelaar, H.L.C.; Dworzanski, J.P.; Kim, M.-G., Field Detection of Bacillus Spore Aerosols with Stand-Alone Pyrolysis-Gas Chromatography-Ion Mobility Spectrometry. *Field Anal. Chem. Technol.* **1999**, 3, pp 315-326.

22. Snyder, A.P.; Maswadeh, W.M.; Tripathi, A.; Dworzanski, J.P. Detection of Gram-Negative Erwinia herbicola Outdoor Aerosols with Pyrolysis-Gas Chromatography-Ion Mobility Spectrometry. *Field Anal. Chem. Technol.* **2000**, 4, pp 111-126.

23. Snyder, A.P.; Tripathi, A.; Maswadeh, W.M.; Ho, J.; Spence, M. Field Detection and Identification of a Bioaerosol Suite by Pyrolysis-Gas Chromatography-Ion Mobility Spectrometry. *Field Anal. Chem. Technol.* **2001**, 5, pp 190-204.

24. Griest, W.H.; Wise, M.B.; Hart, K.J.; Lammert, S.A.; Thompson, C.V.; Vass, A.A. Biological Agent Detection and Identification by the Block II Chemical Biological Mass Spectrometer. *Field Anal. Chem. Technol.* **2001**, 5, pp 177-184.

25. Mukoda, T.J.; Todd, L.A.; Sobsey, M.D. PCR and Gene Probes for Detecting Bioaerosols. *J. Aerosol Sci.* **1994**, 25, pp 1523-1532.

26. Alvarez, A.J.; Buttner, M.P.; Toranzos, G.A.; Dvorsky, G.A.; Toro, A.; Heikes, T.B.; Mertikas-Pifer, L.E.; Stetzenbach, L.D. Use of Solid-Phase PCR for Enhanced Detection of Airborne Microorganisms. *Appl. Environ. Microbiol.* **1994**, 60, pp 374-376.

27. Williams, R.H.; Ward, E.; McCartney, H.A. Methods for Integrated Air Sampling and DNA Analysis for Detection of Airborne Fungal Spores. *Appl. Environ. Microbiol.* **2001**, 67, pp 2453-2459.

28. Speight, S.E.; Hallis, B.A.; Bennett, A.M.; Benbough, J.E. Enzyme-Linked Immunosorbent Assay for the Detection of Airborne Microorganisms Used in Biotechnology. *J. Aerosol. Sci.* **1997**, 28, pp 483-492.

29. Maswadeh, W.M.; Snyder, A.P. Hand-held Temperature Programmable Modular Gas Chromatograph, U. S. Patent 5,856,616, January 5, 1999.

30. Eiceman, G.A.; Karpas, Z. *Ion Mobility Spectrometry*, Chapter 2, CRC Press, Inc.: Boca Raton, FL, 1994.

31. Eiceman, G.A. Advances in Ion Mobility Spectrometry. *Crit. Rev. Anal. Chem.* **1991**, 22, pp 471-480.

32. Vervaet, C.; Byron, P.R. Polystyrene Microsphere Spray Standards Based on CFC-Free Inhaler Technology. *J. Aerosol. Med.* **2000**, 13, pp 105-115.

33. Snyder, A.P.; Thornton, S.N.; Dworzanski, J.P.; Meuzelaar, H.L.C. Detection of the Picolinic Acid Biomarker in Bacillus Spores Using a Potentially Field-Portable Pyrolysis-Gas Chromatography-Ion Mobility Spectrometry System. *Field Anal. Chem. Technol.* **1996**, 1, pp 49-58.

34. Gould, G.W.; Hurst, A. *The Bacterial Spore*. Academic Press: New York, 1969.

35. Malinowski, E.R., and Howery, D.G. *Factor Analysis in Chemistry*, Wiley-Interscience: New York, 1980.

36. Snyder, A.P.; Maswadeh, W.M.; Eiceman, G.A.; Wang, Y.-F.; Bell, S.E. Multivariate Statistical Analysis Characterization of Application-Based Ion Mobility Spectra. *Anal. Chim. Acta.* **1995**, 316, pp 1-14.

Blank

GLOSSARY

ASCII	American Standard Code for Information Interchange
BG	*Bacillus subtilis Variant Niger* bacteria
CAM	Chemical Agent Monitor
EH	*Erwinia herbicola* bacteria
MS	mass spectrometry
OV	ovalbumin protein
PCMCIA	personal computer memory card international association
PCR	polymerase chain reaction
Py-GC-IMS	pyrolysis-gas chromatography-ion mobility spectrometry
RIP	reactant ion peak
TIC	total ion current
TiO_2	titanium dioxide
UV-VIS	